



Published in final edited form as:

Arterioscler Thromb Vasc Biol. 2015 November ; 35(11): 2354–2365. doi:10.1161/ATVBAHA.115.305775.

Mechanisms of Amplified Arteriogenesis in Collateral Artery Segments Exposed to Flow Direction Reversal

Joshua L. Heuslein^{1,*}, Joshua K. Meisner^{1,*}, Xuanyue Li¹, Ji Song¹, Helena Vincentelli¹, Ryan J. Leiphart¹, Elizabeth G. Ames^{1,2}, and Richard J. Price^{1,3,4}

¹Department of Biomedical Engineering, University of Virginia, Charlottesville, Virginia

²Department of Molecular Physiology and Biological Physics, University of Virginia, Charlottesville, Virginia

³Department of Radiology, University of Virginia, Charlottesville, Virginia

⁴Department of Radiation Oncology, University of Virginia, Charlottesville, Virginia

Abstract

Objective—Collateral arteriogenesis, the growth of existing arterial vessels to a larger diameter, is a fundamental adaptive response that is often critical for the perfusion and survival of tissues downstream of chronic arterial occlusion(s). Shear stress regulates arteriogenesis; however, the arteriogenic significance of flow direction reversal, occurring in numerous collateral artery segments after femoral artery ligation (FAL), is unknown. Our objective was to determine if flow direction reversal in collateral artery segments differentially regulates endothelial cell signaling and arteriogenesis.

Approach and Results—Collateral segments experiencing flow reversal after FAL in C57BL/6 mice exhibit increased pericollateral macrophage recruitment, amplified arteriogenesis (30% diameter and 2.8-fold conductance increases), and remarkably permanent (12 weeks post-FAL) remodeling. Genome-wide transcriptional analyses on HUVECs exposed to flow reversal conditions mimicking those occurring in-vivo yielded 10-fold more significantly regulated transcripts, as well as enhanced activation of upstream regulators (NF κ B, VEGF, FGF2, TGF β) and arteriogenic canonical pathways (PKA, PDE, MAPK). Augmented expression of key pro-arteriogenic molecules (KLF2, ICAM-1, eNOS) was also verified by qRT-PCR, leading us to test whether ICAM-1 and/or eNOS regulate amplified arteriogenesis in flow-reversed collateral segments in-vivo. Interestingly, enhanced pericollateral macrophage recruitment and amplified arteriogenesis was attenuated in flow-reversed collateral segments after FAL in ICAM-1^{-/-} mice; however, eNOS^{-/-} mice showed no such differences.

Conclusions—Flow reversal leads to a broad amplification of pro-arteriogenic endothelial signaling and a sustained ICAM-1-dependent augmentation of arteriogenesis. Further

Corresponding Author: Richard J. Price, PhD, Department of Biomedical Engineering, University of Virginia, Box 800759, Health System, Charlottesville, Virginia 22903, Tel: 434-924-0020, Fax: 434-982-3870, rprice@virginia.edu.

*authors contributed equally on this work

Disclosures

None

investigation of the endothelial mechanotransduction pathways activated by flow reversal may lead to more effective and durable therapeutic options for arterial occlusive diseases.

Keywords

arteriogenesis; endothelial cell; peripheral arterial disease; hemodynamics; gene expression

Introduction

The importance of adequate remodeling of pre-existing arterial interconnections to form endogenous collateral bypasses – i.e. arteriogenesis – is highlighted by the extensive link between adequate collateral development and improved outcomes in patients with arterial occlusive disease^{1,2}. However, few clinical trials designed to therapeutically stimulate collateral development have proven successful^{3–6}. This is likely related to the fact that these interventions do not necessarily recapitulate the complex sequence of processes that must be coordinated to achieve functional collateral development^{1,7,8}. These clinical results have led to a re-examination of the basic mechanisms underlying collateral remodeling in the hope of identifying central signaling pathways for better therapeutic development.

As early as 1893, Thoma observed a correlation between vessel diameter and blood flow⁹. We now know the biomechanical forces exerted by blood flow on the endothelium are critical in regulating cell phenotype and blood vessel remodeling^{8,10–14}. Indeed, a key initiating stimulus for arteriogenesis is a change in shear stress⁸. Upon occlusion of a major artery, downstream pressure is reduced, causing an increase in pressure gradient, blood flow, and shear stress along pre-existing collateral arteries that bypass the occlusion. Both the magnitude¹⁵ and duration¹⁶ of increased shear stress determine maximal collateral outgrowth. Collateral artery growth is hypothesized to eventually resolve as the increased outward remodeling reduces shear stress magnitude to a homeostatic “set-point”¹⁷.

Nonetheless, the topological arrangement of collateral arteries in skeletal muscle also dictates that shear stress will vary on a segment-to-segment basis along any given collateral pathway after the occlusion of a major artery. Recently, we applied transillumination based laser speckle flowmetry (LSF) to quantify, for the first time, the in-vivo “segment-to-segment” spatial distribution of collateral artery hemodynamics before and after femoral artery ligation in the mouse ischemic hindlimb, the most widely used model of peripheral arteriogenesis. While shear stress magnitude increased ~2-fold along the length of the collateral vessels in the gracilis adductor muscle, some pre-existing collateral artery segments also experienced a reversal of flow direction after femoral artery ligation¹⁸. In the present study, we tested the hypothesis that a change in flow direction has a profound influence on both arteriogenesis and mechanotransductive endothelial cell signaling.

Materials and Methods

Materials and Methods are available in the online-only Data Supplement.

Results

Planar Polarization Confirms Endothelial Cell Responsiveness to Predicted Flow Directions

Femoral arterial ligation (FAL), performed as previously described¹⁸, was used to induce arteriogenesis in the gracilis adductor muscle collateral arteries. In agreement with previous studies^{19,20}, perfusion measurements of the plantar surface of the foot indicated moderate ischemia immediately post-FAL, followed by a return to full perfusion by day 7 post-FAL (Supplemental Figure I). The position of the ligation along the femoral artery was chosen to yield a change in blood flow direction and magnitude along the length of the two collateral arteries in this muscle. Pre-ligation, blood flows toward a convergence point in the center of the gracilis muscle via the muscular branch artery (also known as the lateral caudal femoral artery) and via the saphenous artery (Figure 1A). FAL causes a decrease in downstream pressure, resulting in increased flow through the gracilis collaterals and a reversal of flow direction in those collateral segments near the saphenous artery (Figure 1A). Using transillumination laser speckle flowmetry (LSF), we recently determined that shear stress magnitude increases 2-fold in both the muscular and saphenous collateral entrance regions 30 minutes post-FAL. Additionally, we confirmed the predicted flow directions in this ligation scheme through observation of circulating fluorescent microspheres during intravital imaging¹⁸.

To further confirm endothelial cell responsiveness to the change in flow direction, we characterized endothelial cell planar polarization (PCP) in the gracilis collateral arteries by examination of the perinuclear position of the Golgi apparatus (GA) with respect to predicted flow direction both pre-FAL and 24hrs post-FAL (Figure 1B–E). At baseline, endothelial cells at the collateral entrance regions were primarily polarized toward their respective upstream directions (Figures 1B and 1D), while the central regions of the gracilis collateral arteries showed no significant polarization. By 24 hours post-FAL, however, most of the endothelial cells in both the central and saphenous entrance regions repolarized toward the muscular branch artery, instead of the saphenous artery (Figure 1B and 1E).

Arteriogenesis is Enhanced in Collateral Artery Segments Exposed to Flow Reversal after FAL

To determine if flow direction reversal affects arteriogenesis, we measured luminal collateral diameter in the muscular branch and saphenous artery entrance regions using vascular casting (Figure 2A). After 24 hours, neither region demonstrated significant luminal expansion compared to the unligated control limb. By day 3, however, both the saphenous (reversed) and muscular (non-reversed) regions underwent significant ($p < 0.001$ and $p = 0.04$ respectively) luminal expansion compared to unligated controls ($58.8 \pm 8.5\%$ and $19.9 \pm 4.7\%$ increases respectively). Furthermore, the saphenous (i.e. flow-reversed) segment began to exhibit a significant ($p = 0.004$) enhancement in luminal diameter when compared to the non-reversed muscular branch. Luminal diameter in both reversed and non-reversed regions increased further by day 7 post-ligation ($93.7 \pm 9.1 \mu\text{m}$ and $70.7 \pm 6.1 \mu\text{m}$ within saphenous and muscular branch regions respectively), but thereafter remained constant through 12 weeks post-FAL ($91.6 \pm 3.3 \mu\text{m}$ and $75.2 \pm 5.2 \mu\text{m}$). At both 1 and 12 weeks post-

FAL, luminal diameter was significantly greater in the flow-reversed saphenous region when compared to the non-reversed muscular branch region ($p=0.01$) (Figure 2B). The time course of arteriogenesis matched well with the laser Doppler reperfusion measurements (Supplemental Figure I), where resting foot perfusion returned to baseline around 5 days post-ligation, with no further increases in reperfusion.

Cross-sectional analysis of the collateral artery entrance regions was used to confirm whole-mount diameter measurements and determine whether wall mass was also increased in flow reversed segments (Figure 2C). Both reversed and non-reversed regions showed significantly increased luminal diameter, wall area, and wall thickness versus their respective unligated controls at 7 days post-FAL (Figure 2C–F). In confirmation of the whole mount vascular cast analysis, we observed an enhancement of luminal diameter in the flow-reversed saphenous region ($36.7\pm 2.3\%$ vs. non-reversed muscular region, $p<0.01$) at day 7. Wall area in the flow reversed region was also significantly increased at day 7 when compared to the non-reversed region ($47.9\pm 5.8\%$, $p<0.05$). These significant increases in luminal diameter and wall area in flow-reversed regions were maintained up to 12 weeks after FAL (Figure 2D–E).

FAL Does Not Elicit Regional Differences in Hypoxia in Gracilis Adductor Muscles

We next examined whether hypoxia in the gracilis adductor muscle could be contributing to the observed spatial differences in arteriogenesis between the flow-reversing and non-reversing regions. Twenty-four hours post-FAL, we observed no regional differences in gracilis muscle hypoxia as determined by pimonidazole-HCl immunolabeling (Supplemental Figure IIA–C). Other indicators of tissue hypoxia, namely muscle fiber atrophy (Supplemental Figure IIE) and angiogenesis (Supplemental Figure IIF), were also found to be unchanged in the flow-reversed saphenous region when compared to both non-reversed muscular branch regions and unligated controls.

Enhanced Arteriogenesis in Flow-Reversed Segments Occurs Independent of Position

To verify that enhanced arteriogenesis in response to flow-reversal can occur in other collateral regions, we employed a muscular branch ligation (MBL) scheme that creates flow reversal in the muscular branch collateral region, instead of in the saphenous region (Supplemental Figure IIIA). Flow direction reversal was confirmed via reorientation of the perinuclear position of the Golgi apparatus toward the saphenous entrance region (Supplemental Figure IIIB–C). Flow-reversed collateral segments in the muscular branch region exhibited significant luminal growth when compared to non-reversing segments in the saphenous region at 14 days post-MBL ($36.2\pm 4.9\%$ vs. non-reversed, $p<0.01$) (Supplemental Figure IIID–E).

HUVECs Exhibit Directional Responsiveness to Simulated Femoral Artery Ligation

To investigate the influence of FAL-elicited hemodynamic changes on EC signaling, HUVECs were exposed to biomimetic changes in relative shear stress magnitude and/or direction, as previously determined by transillumination LSF¹⁸ (Figure 3A). A value of 15 dynes/cm² shear stress was chosen as a baseline shear stress²¹. Preconditioning for 24 hours at this baseline shear stress was used to establish endothelial cell alignment and PCP,

thereby mimicking the in-vivo baseline state. FAL was then simulated by a step-wise 100% increase in shear stress, in either the same direction or in the opposite direction, to mimic shear stress changes occurring in the muscular branch (non-reversed) and saphenous artery (reversed) entrance regions, respectively (Figure 3A). Consistent with in-vivo observations, HUVECs aligned with the flow direction and showed an upstream polarization of the GA with respect to the nucleus in control plates maintained at 15 dynes/cm². Upstream polarization was maintained (at 2 hours) or enhanced (at 6 hours) with a non-reversing, step-wise increase in shear stress (Supplemental Figure IV). However, when shear direction was reversed, endothelial cells transitioned from the PCP induced by preconditioning toward the new upstream direction within 6 hours (Supplemental Figure IV). Using HUVECS, we confirmed that GA perinuclear position matches well with MTOC perinuclear position (Supplemental Figure IV). These data demonstrate sensitivity to directional change in shear stress in HUVECs similar to that seen in-vivo, with complete re-orientation of PCP toward the new upstream direction within 6 hours after reversal.

Flow Reversal Broadly Enhances the Arteriogenic Transcriptional Profile

To then comprehensively determine how a change shear stress magnitude, coupled with a change in flow direction, activates pro-arteriogenic endothelial cell mechanosignaling pathways, we performed genome-wide, microarray transcriptional analysis on HUVECs exposed to the simulated femoral arterial ligation (“FAL”) shear stress protocol (Figure 3A). The 6 hour post-FAL time-point was chosen because PCP reorientation is complete and robust transcriptional changes in response to a stepwise shear stress increase have been previously reported²². Using a false discovery rate (FDR) for significance of <0.10 obtained through the Robust Multiarray Average (RMA) algorithm, HUVECs exposed to a flow-direction reversal showed an ~10-fold greater number of transcripts (reversed versus control, RvC, Supplemental Table IIIA) compared to HUVECS exposed to increased shear stress magnitude only (non-reversed versus control, NvC, Supplemental Table IIIB) (Figure 3B). While flow reversal induced significant changes in more transcripts, the genes altered by a shear stress increase alone (NvC) demonstrated a similar expression pattern as those also exposed to a reversal in shear stress direction (RvC). When the expression of the 537 genes with FDR<0.1 (in NvC and/or RvC comparisons) was compared in both NvC and RvC groups, 97.4% were altered in the same expression direction; i.e. genes that were up-regulated in reversed conditions were also up-regulated in non-reversed conditions and vice versa (Figure 3C). Interestingly, within this overlap, 93.9% of genes were altered to a greater degree in the reversed condition than in the non-reversed condition (Figure 3C). Of the 2.6% of genes exhibiting regulation in opposing directions between reversed and non-reversed conditions, all had a fold change <0.1 and an FDR>0.88 in the non-reversed group. With the changes of expression occurring in similar directions from the control state, there were no significant differences between reversal and non-reversal expression levels with an FDR<0.20. An *a priori* selection of 7 genes was used to validate the microarray results through real-time quantitative PCR (Table 1). All genes showed similar expression patterns and significance between microarray and RT-PCR measurements. However, the increased sensitivity of RT-PCR yielded significant differences between reversal and non-reversal conditions for ICAM-1, eNOS, and KLF2, all of which are known to play key roles in

arteriogenesis^{19,23,24} and are established as being sensitive to arterial levels of shear stress^{25–36}.

Initial assessment of activated molecular functions was conducted through gene ontology analysis³⁷ to assess over-representation of molecular pathways. The 500 most significantly regulated genes based on p-value ranking for increased shear stress, with and without flow reversal, as compared to control were used to investigate the broad functional processes involved in both conditions (Supplemental Table I). Oxidoreductase activity was the only significantly enriched molecular function in the case of the non-reversed increased shear stress (Supplemental Figure VA). However, with the addition of a change in shear stress direction, there was activation of multiple molecular functions including: reelin receptor activity, RNA pol II promoter transcription factors, cAMP phosphodiesterase activity, and GTPase regulation (Supplemental Figure VB, Supplemental Table I).

NFκB as a Predicted Upstream Regulator of Gene Expression Patterns in Flow Reversed Conditions

Additional function annotation, clustering, and analysis of predicted upstream regulators were performed with the Ingenuity Pathways Analysis software. Analysis of predicted upstream transcriptional regulators for all genes with FDR<0.1 identified many of the known signaling pathways involved in arteriogenesis including activation of the NFκB pathway^{38–40} (Table 2) as well as growth factors [e.g. VEGF^{41,42}, HGF^{43,44}, TGFβ⁴⁵, FGF2^{46,47}], MAPK signaling^{16,48,49}, and PI3K signaling⁵⁰ (Supplemental Table IIA). Across all of these signaling pathways and upstream regulators, a clear activation was only apparent under the reversed direction condition.

Further clustering of expression changes of all genes with FDR<0.1 along canonical pathways showed activation of several key pathways known to be involved in arteriogenesis, including cGMP signaling^{19,51}, protein kinase A signaling^{52,53}, MAPK signaling^{16,48,49}, and cell-cell junction signaling^{54,55} (Figure 3D–G, Supplemental Table IIB). HUVECs exposed to a flow reversal showed much stronger activation of these canonical pathways versus those exposed to non-reversed conditions (Supplemental Table IIB).

Amplified Arteriogenesis in Flow-Reversed Collateral Depends on ICAM-1

One pathway of particular interest from our Ingenuity Pathway Analysis of upstream regulators (Table 2) was the NFκB-ICAM-1 pathway. NFκB is a mechanosensitive transcription factor that regulates arteriogenesis^{40,56} through ICAM-1^{26,57} dependent monocyte/macrophage recruitment²³. To further investigate the NFκB- ICAM-1 pathway, we confirmed increased NFκB activity in HUVECs 1 hour after exposure to our in vitro “FAL” using a luciferase reporter assay (Figure 4A). Moreover, ICAM-1 mRNA expression was already shown to be increased (35%) under flow reversal conditions as determined from our *a priori* RT-PCR screen of known pro-arteriogenic genes (Table 1, Figure 4B). Western blotting confirmed its up-regulation (38.5%) at the protein level 6 hours after simulated FAL (Figure 4C). Additionally, flow reversal led to increased pro-arteriogenic function in-vitro as determined by increased monocyte adhesion to flow-conditioned HUVECs (Figure 4D–F). Furthermore, using a siRNA knockdown of ICAM-1, this increase in monocyte adhesion

was found to be ICAM-1 dependent (Figure 4D–F). We also determined there was over a 2-fold increase in pericollateral Mac3⁺ macrophages 3 days post-FAL in collateral segments of C57BL/6 mice that experienced flow-reversal (6.53±1.00 and 3.12±0.47 cells in reversed and non-reversed pericollateral regions, respectively), as seen in Figure 5A–B. This increase in pericollateral macrophage density was attenuated in flow-reversed segments of ICAM-1^{-/-} mice as there was no significant difference in reversed vs. non-reversed collateral segments (2.33±0.44 and 1.67±0.31 cells in reversed and non-reversed pericollateral regions, respectively, p=0.34) (Figure 5A–B).

Based on these findings, we next tested whether ICAM-1 was necessary for amplified arteriogenesis in flow-reversed collateral segments in-vivo by applying FAL to ICAM-1^{-/-} mice. There were no significant differences between ICAM-1 null mice and WT in diameters of collateral segments in unligated limbs. The muscular, non-reversed collateral segments in ICAM-1^{-/-} mice were not significantly different than those in WT mice (p=0.11). However, deletion of ICAM-1 reduced the amplified collateral growth that occurs in collateral segments of WT mice exposed to a flow reversal (p=0.017). Importantly, in these ICAM-1^{-/-} mice, we also observed no significant differences in diameter between reversing and non-reversing collateral segments at 14 days post-FAL (66.5±5.95 and 61.2±6.05 respectively, p=0.48). Therefore the amplified arteriogenesis that occurs in flow reversed segments of WT mice (1.24±0.12 fold-change, reversed vs. non-reversed) is attenuated in ICAM-1 null mice (1.08±0.14 fold-change, reversed vs. non-reversed), demonstrating that ICAM-1 is necessary for the amplified response in segments exposed to a reversal in flow direction (Figure 5C–D).

Our transcriptional profiling data and *a priori* RT-PCR screen also suggested a potential role for the KLF2/eNOS pathway. We first determined that KLF2 and eNOS mRNA expression were enhanced by 33% and 83%, respectively, in HUVECs exposed to FAL-simulated flow-reversal (Supplemental Figure VIA–B). Phosphorylated (S1177) eNOS protein expression was also increased under flow reversal conditions (Supplemental Figure VIC). To then test whether eNOS was required for amplified arteriogenesis in flow-reversed collateral segments in-vivo, we applied FAL to eNOS^{-/-} mice. When all regional measurements of collateral growth are binned together, we observe a 17% decrease in arteriogenesis in eNOS^{-/-} mice compared to wild-type (eNOS^{-/-} 67.67±3.38µm; C57BL/6: 81.37±4.54µm; p<0.05) (Supplemental Figure VIE). If each collateral region is analyzed separately, luminal diameter in non-reversing, muscular collateral artery segments was significantly reduced in eNOS^{-/-} mice compared to wild-type mice (eNOS^{-/-} 52.4±4.1 µm; C57BL/6: 72.5±5.0 µm, p<0.05), but not in the flow-reversing, saphenous segments (eNOS^{-/-} 82.6±3.6µm; C57BL/6: 90.2±6.2µm, p = 0.463) (Supplemental Figure VIF). However, when each region was normalized to its respective unligated control, amplified luminal growth in flow-reversing segments was maintained in eNOS^{-/-} mice, indicating that this enhanced remodeling response is independent of eNOS (Supplemental Figure VIG).

Discussion

We report here a comprehensive, genome-wide, and direct mapping of mechanotransductive endothelial cell signaling pathway activation to a uniquely amplified and sustained in-vivo

arteriogenesis response. We first used endothelial cell planar polarization as a marker to confirm endothelial cell responsiveness to the change in flow direction in the gracilis adductor collateral arteries following femoral arterial ligation (Figure 1). We then determined that collateral artery segments that are exposed to both an increase in shear stress magnitude and a reversal of flow direction exhibit markedly amplified arteriogenesis when compared to collateral artery segments exposed to increased shear stress magnitude alone (Figure 2). Genome-wide transcriptional profiling of HUVECs exposed to a biomimetic “reversed-flow + increased shear stress magnitude” waveform yielded a ~10-fold increase in significantly regulated transcripts when compared to HUVECs exposed to increased shear-stress alone. Indeed, this stimulus acts as a broad amplifier of transcriptional activation (Figure 3), including a set of potent arteriogenesis regulators (eNOS, ICAM-1, and KLF-2) that were then confirmed by RT-PCR (Table 1). Further, Ingenuity Pathways Analysis indicated activation of a number of important canonical arteriogenesis pathways and upstream regulators, notably NF κ B (Figure 4, Table 2). After confirming that the NF κ B-ICAM-1 pathway was activated in HUVECs exposed to flow-reversal, we showed the increased monocyte adhesion to HUVECs exposed to flow reversal was abrogated by knockdown of ICAM-1 (Figure 4). Finally, we demonstrated that enhanced pericollateral Mac3⁺ macrophage density and amplified arteriogenesis in flow-reversed collateral segments of WT mice was attenuated in ICAM-1^{-/-} mice, indicating that this amplified arteriogenic response is ICAM-1 dependent (Figure 5).

Flow Reversal as an Independent Stimulus Leading to Amplified Arteriogenesis

Our ability to link amplified arteriogenesis to a unique hemodynamic stimulus (i.e. flow-reversal with increase shear stress magnitude) was facilitated by the development of a laser speckle flowmetry approach for mouse hindlimb collaterals¹⁸. We developed that approach because, despite the known importance of hemodynamic stimuli in driving collateral development, there was a surprising lack of quantitative data on the hemodynamic changes within these arteries. This is likely due to both the small size of the arteries (<100 μ m) and the fact that different surgical models elicit arteriogenesis along different collateral pathways². Using laser speckle flowmetry¹⁸, we determined the occurrence of at least three distinct hemodynamic conditions in these collateral vessels: a non-reversing increase in shear stress near the feeding entrance to the collateral loop, an increase in shear stress from low/oscillating flow to sustained high shear stress at the central anastomotic region, and an increase in shear stress but in a reversed direction at the downstream outlet back into the occluded arterial tree. In this study, we only considered the two entrance regions because they experience the same step increase in relative shear stress magnitude after FAL, thereby permitting isolation of the influence of flow-reversal.

Nonetheless, we also had to consider that hypoxia in flow-reversing regions could be contributing to amplified arteriogenesis. Indeed, previous studies using saphenous artery excision models that elicit severe ischemia have suggested a role for hypoxia and metabolic signaling in the arteriogenic response^{58,59} and observed spatial differences in capillary density in the adductor muscles as a marker of ischemic response⁶⁰. Thus, we examined the potential role of hypoxia in eliciting spatial differences in arteriogenesis between the flow-reversing and non-reversing regions. In our study, pimonidazole-HCl immunolabeling

revealed no signs of regional differences in hypoxia at 24 hours post-FAL (Supplemental Figure IIA–C). Consistent with previous findings for the gracilis muscle using a similar, milder (i.e. far less ischemic) FAL scheme⁶¹, there was no evidence of angiogenesis in either the muscular branch or saphenous artery regions (Supplemental Figure IIF). As another indirect measure of tissue ischemia, muscle fiber size in the gracilis muscle showed no evidence of atrophy in either the muscular branch or saphenous artery regions (Supplemental Figure IIE). Thus, our results are consistent with previous studies using similar hindlimb models in which arteriogenesis proceeds independent of a hypoxic stimulus^{61–63}.

Additionally, to confirm that flow-reversal can elicit amplified arteriogenesis independent of longitudinal position along a given collateral, we employed the MBL model to induce flow-direction reversal in the muscular branch entrance region, instead of in the saphenous region (Supplemental Figure III). With this ligation scheme, we observed both endothelial cell repolarization and amplified arteriogenesis in the muscular branch region of the collaterals, thereby establishing that this amplified arteriogenesis response is indeed not unique to the saphenous collateral region. In all, we conclude that flow-direction reversal is a novel, independent stimulus for arteriogenesis.

Endothelial Cell Sensing of Shear Stress Magnitude and Reversal

One motivation for the current study is that the endothelial response to increased shear stress from a pre-conditioned baseline state is not well-studied. In perhaps the most closely related study, a nearly 20x reduction in the number of genes that are sensitive to a step-wise increase in shear stress from a pre-conditioned baseline was observed when compared to a step change from static conditions (i.e. 86 versus 1838)²². Our data matches this previous study well, as only 48 genes were significantly altered (FDR<0.1) at 6 hours after a non-reversed 100% step increase in shear stress. This implies that gene expression changes induced by the application of laminar shear stress from static culture are not wholly predictive of gene expression changes occurring in the more physiological scenario of a step increase in shear stress from a non-zero baseline²².

Studies incorporating non-reciprocating directional flow changes indicate that shear stress reversal from baseline has a disproportionate impact on responses such as permeability⁶⁴, which is a hallmark in the initiation of arteriogenesis⁸, and intracellular calcium⁶⁵. Because pre-conditioned, flow-adapted endothelial cells align with flow direction and incline their cell-cell junctions to reduced tension, they experience a dramatic increase in cell to cell tension when faced with a sudden flow reversal. This leads to a disproportionate response in endothelial cell signaling⁶⁵. Interestingly, a step change in shear stress magnitude from a preconditioned level of 15 dyne/cm² to a very low level of 2.5 dynes/cm² with a reversal in flow direction elicits a disproportionately larger transcriptional response (of a similar pattern) than a step increase in shear stress (+10 dynes/cm²) in the same direction⁶⁶. Our data demonstrate that adding flow-reversal to a 2x increase in shear stress magnitude elicits a 10-fold increase in transcriptional activation. Moreover, in addition to broadly modulating the endothelial shear stress response, a change in flow direction relative to an endothelial cell's morphological and cytoskeletal axes can stimulate activation of distinct pathways⁶⁷.

Together, these data suggest that EC responsiveness to altered shear stress is highly dependent on initial conditions. For the specific case of shear signaling for arteriogenesis, consideration of the initial hemodynamic conditions across a given collateral network is especially significant.

Endothelial Cell Repolarization and Signaling for Amplified Arteriogenesis

In this study, endothelial cell planar polarization was used simply as a marker of endothelial cell responsiveness to a change in flow direction. To date there has been no direct functional link between endothelial planar (re)polarization and arteriogenesis; however our results offer an opportunity to explore this linkage. Indeed many molecular pathways that are activated by flow reversal in our study, such as small GTPase signaling (Supplemental Figure V) and ICAM-1 (Figure 4), regulate both planar cell polarization^{68–71} and arteriogenesis^{16,23,72}, raising the hypothesis that endothelial cell polarization may play a significant role in collateral artery remodeling. However, the functional consequence(s) of endothelial cell repolarization remains to be determined and future work could investigate the mechanistic role(s) of endothelial planar polarization in arteriogenesis.

Complex Role of eNOS Signaling in Arteriogenesis

Our transcriptional profiling and qRT-PCR studies led us to hypothesize that ICAM-1 and eNOS are important regulators of amplified arteriogenesis in flow-reversed collaterals. Here, we demonstrated ICAM-1 is necessary for enhanced monocyte/macrophage recruitment and augmented arteriogenesis in flow-reversed collateral segments. Together, these results are consistent with the previously demonstrated vital role for ICAM-1 in arteriogenesis through its regulation of monocyte/macrophage recruitment²³.

While our ICAM-1^{-/-} studies show attenuation of this amplified arteriogenic response, our eNOS^{-/-} studies do not. The role of eNOS and/or NO in arteriogenesis is fairly well-studied, yet still difficult to interpret. While eNOS and NO regulate arteriogenesis in more severe excision hindlimb models^{73,74} and in training models⁷⁵, no significant defects in arteriogenesis were reported for eNOS^{-/-} mice three weeks after induction of a less ischemic femoral ligation model⁷⁶. For our data set, if luminal diameters at either end of the collateral are averaged, we observed a moderate decrease in arteriogenesis in eNOS^{-/-} mice compared to wild-type. Given that eNOS can affect the baseline network configuration and maintenance¹⁹, we normalized the diameters of the ligated muscular branch and saphenous regions to their respective unligated controls (Supplemental Figure VIG). Using this analysis, we observe that the enhanced arteriogenesis caused by flow-reversal is eNOS independent potentially due to the ability to compensate for the loss of eNOS with other NOS subtypes.

Implications for Understanding Shear Stress Set-Point

Finally, our results may have important implications for our understanding of the so-called homeostatic “set-point” for constant shear stress in the arterial circulation. In 1926, Murray put forth his “principle of minimum work”, a consequence of which is that shear stress is maintained at a relatively constant level throughout the arterial vasculature¹⁷. In support of this concept, there appears to be a homeostatic wall shear stress magnitude (i.e. set-point) at

which endothelial cells become quiescent and vessels maintain a steady state luminal diameter⁷⁷. Little is known, however, about how this set-point is achieved or maintained at the molecular signaling level. In our FAL model, if we assume Poiseuille flow, apply mass conservation, and consider that the luminal diameter at the distal end (i.e. saphenous region) of the collateral is 22% greater than the luminal diameter in the proximal end (i.e. muscular branch region) at 12 weeks post-FAL (Figure 2B), we estimate that the new steady-state shear stress in the saphenous region is reduced by at least 45% from pre-FAL levels. Thus, in essence, the flow-reversal stimulus effectively resets the set-point for constant shear stress. We posit that further examination of this response could uncover molecular regulators of the shear stress set-point and/or provide clues for generating sustained therapeutic arteriogenic responses via set-point adjustment(s).

Supplementary Material

Refer to Web version on PubMed Central for supplementary material.

Acknowledgments

The authors would like to thank Dr. Stephen Turner (University of Virginia Bioinformatics Core) for help in processing and analysis of the microarray data and the University of Virginia Research Histology Core (under the direction of Sheri VanHoose) for histological tissue processing. The authors would also like to thank Dr. Brett Blackman for material support and guidance.

Sources of Funding

This material is based upon work supported by the National Science Foundation Graduate Research Fellowship Program under Grant No. NSF DGE-1315231 (JLH). Additional funding sources: American Heart Association awards 09PRE2060385 (JKM) and 10GRNT3490001 (RJP), and NIH grants T32-GM007267 (JKM), T32-HL007284 (JKM and JLH), R21-HL098632 (RJP).

Abbreviations

LSF	laser speckle flowmetry
FAL	femoral arterial ligation
MBL	muscular branch ligation
EC	endothelial cell
HUVEC	human umbilical vein endothelial cells
NvC	non-reversed vs. control
RvC	reversed vs. control
PCP	planar cell polarization
MTOC	microtubule organizing center
GA	Golgi apparatus

References

1. Van Royen N, Piek JJ, Schaper W, Fulton WF. A critical review of clinical arteriogenesis research. *J Am Coll Cardiol.* 2009; 55:17–25. [PubMed: 20117358]

2. Ziegler MA, Distasi MR, Bills RG, Miller SJ, Alloosh M, Murphy MP, Akingba AG, Sturek M, Dalsing MC, Unthank JL. Marvels, mysteries, and misconceptions of vascular compensation to peripheral artery occlusion. *Microcirculation*. 2010; 17:3–20. [PubMed: 20141596]
3. Ripa RS, Jørgensen E, Wang Y, Thune JJ, Nilsson JC, Søndergaard L, Johnsen HE, Køber L, Grande P, Kastrup J. Stem cell mobilization induced by subcutaneous granulocyte-colony stimulating factor to improve cardiac regeneration after acute ST-elevation myocardial infarction: result of the double-blind, randomized, placebo-controlled stem cells in myocardial infarction. *Circulation*. 2006; 113:1983–92. [PubMed: 16531621]
4. Subramaniam V, Waller EK, Murrow JR, Manatunga A, Lonial S, Kasirajan K, Sutcliffe D, Harris W, Taylor WR, Alexander RW, Quyyumi AA. Bone marrow mobilization with granulocyte macrophage colony-stimulating factor improves endothelial dysfunction and exercise capacity in patients with peripheral arterial disease. *Am Hear J*. 2009; 158:53–60.
5. Simons M. Pharmacological treatment of coronary artery disease with recombinant fibroblast growth factor-2: double-blind, randomized, controlled clinical trial. *Circulation*. 2002; 105:788–793. [PubMed: 11854116]
6. Kusumanto YH, van Weel V, Mulder NH, Smit AJ, van den Dungen JJAM, Hooymans JMM, Sluiter WJ, Tio RA, Quax PHA, Gans ROB, Dullaart RPF, Hospers GAP. Treatment with intramuscular vascular endothelial growth factor gene compared with placebo for patients with diabetes mellitus and critical limb ischemia: a double-blind randomized trial. *Hum Gene Ther*. 2006; 17:683–91. [PubMed: 16776576]
7. Meisner JK, Price RJ. Spatial and temporal coordination of bone marrow-derived cell activity during arteriogenesis: regulation of the endogenous response and therapeutic implications. *Microcirculation*. 2010; 17:583–599. [PubMed: 21044213]
8. Schaper W. Collateral circulation: past and present. *Basic Res Cardiol*. 2009; 104:5–21. [PubMed: 19101749]
9. Scholz D, Schaper W. Preconditioning of arteriogenesis. *Cardiovasc Res*. 2005; 65:513–23. [PubMed: 15639491]
10. Langille BL, O'Donnell F. Reductions in arterial diameter produced by chronic decreases in blood flow are endothelium-dependent. *Science* (80-). 1986; 231:405–407.
11. Moraes F, Paye J, Mac Gabhann F, Zhuang ZW, Zhang J, Lanahan AA, Simons M. Endothelial cell-dependent regulation of arteriogenesis. *Circ Res*. 2013; 113:1076–86. [PubMed: 23897694]
12. Davies PF. Flow-mediated endothelial mechanotransduction. *Physiol Rev*. 1995; 75:519–560. [PubMed: 7624393]
13. Garcia-Cardeña G, Comander J, Anderson KR, Blackman BR, Gimbrone MA. Biomechanical activation of vascular endothelium as a determinant of its functional phenotype. *Proc Natl Acad Sci U S A*. 2001; 98:4478–85. [PubMed: 11296290]
14. Topper JN, Gimbrone MA. Blood flow and vascular gene expression: fluid shear stress as a modulator of endothelial phenotype. *Mol Med Today*. 1999; 5:40–6. [PubMed: 10088131]
15. Schierling W, Troidl K, Mueller C, Troidl C, Wustrack H, Bachmann G, Kasprzak PM, Schaper W, Schmitz-Rixen T. Increased intravascular flow rate triggers cerebral arteriogenesis. *J Cereb blood flow Metab*. 2009; 29:726–37. [PubMed: 19142189]
16. Eitenmüller I, Volger O, Kluge A, Troidl K, Barancik M, Cai W-J, Heil M, Pipp F, Fischer S, Horrevoets AJG, Schmitz-Rixen T, Schaper W. The range of adaptation by collateral vessels after femoral artery occlusion. *Circ Res*. 2006; 99:656–62. [PubMed: 16931799]
17. Murray CD. The physiological principle of minimum work: I. The vascular system and the cost of blood volume. *Proc Natl Acad Sci U S A*. 1926; 12:207–214. [PubMed: 16576980]
18. Meisner JK, Niu J, Sumer S, Price RJ. Trans-illuminated laser speckle imaging of collateral artery blood flow in ischemic mouse hindlimb. *J Biomed Opt*. 2013; 18:096011. [PubMed: 24045691]
19. Dai X, Faber JE. Endothelial nitric oxide synthase deficiency causes collateral vessel rarefaction and impairs activation of a cell cycle gene network during arteriogenesis. *Circ Res*. 2010; 106:1870–81. [PubMed: 20431061]
20. Distasi MR, Case J, Ziegler MA, Dinauer MC, Yoder MC, Haneline LS, Dalsing MC, Miller SJ, Labarrere CA, Murphy MP, Ingram DA, Unthank JL. Suppressed hindlimb perfusion in *Rac2*^{-/-}

- and *Nox2*^{-/-} mice does not result from impaired collateral growth. *Am J Physiol Hear Circ Physiol.* 2009; 296:H877–86.
21. Chiu J-J, Chien S. Effects of disturbed flow on vascular endothelium: pathophysiological basis and clinical perspectives. *Physiol Rev.* 2011; 91:327–87. [PubMed: 21248169]
 22. Zhang J, Friedman MH. Adaptive response of vascular endothelial cells to an acute increase in shear stress magnitude. *Am J Physiol Hear Circ Physiol.* 2012; 302:H983–991.
 23. Hoefler IE, van Royen N, Rectenwald JE, Deindl E, Hua J, Jost M, Grundmann S, Voskuil M, Ozaki CK, Piek JJ, Buschmann IR. Arteriogenesis proceeds via ICAM-1/Mac-1- mediated mechanisms. *Circ Res.* 2004; 94:1179–85. [PubMed: 15059933]
 24. Mack PJ, Zhang Y, Chung S, Vickerman V, Kamm RD, García-Cardena G. Biomechanical regulation of endothelium-dependent events critical for adaptive remodeling. *J Biol Chem.* 2009; 284:8412–20. [PubMed: 19047056]
 25. Morigi BM, Zoja C, Figliuzzi M, Foppolo M, Micheletti G, Bontempelli M, Saronni M, Remuzzi G, Remuzzi A. Fluid shear stress modulates surface expression of adhesion molecules by endothelial cells. *Blood.* 1995; 85:1696–1703. [PubMed: 7535583]
 26. Nagel T, Resnick N, Atkinson WJ, Dewey CF, Gimbrone MA. Shear stress selectively upregulates intercellular adhesion molecule-1 expression in cultured human vascular endothelial cells. *J Clin Invest.* 1994; 94:885–891. [PubMed: 7518844]
 27. Scholz D, Ito W, Fleming I, Deindl E, Sauer A, Wiesnet M, Busse R, Schaper J, Schaper W. Ultrastructure and molecular histology of rabbit hind-limb collateral artery growth (arteriogenesis). *Virchows Arch.* 2000; 436:257–70. [PubMed: 10782885]
 28. Malek AM, Jiang L, Lee I, Sessa WC, Izumo S, Alper SL. Induction of nitric oxide synthase mRNA by shear stress requires intracellular calcium and G-protein signals and is modulated by PI 3 kinase. *Biochem Biophys Res Commun.* 1999; 254:231–42. [PubMed: 9920763]
 29. Blackman BR, García-Cardena G, Gimbrone MA. A new in vitro model to evaluate differential responses of endothelial cells to simulated arterial shear stress waveforms. *J Biomech Eng.* 2002; 124:397. [PubMed: 12188206]
 30. Davis ME, Grumbach IM, Fukai T, Cutchins A, Harrison DG. Shear stress regulates endothelial nitric-oxide synthase promoter activity through nuclear factor kappaB binding. *J Biol Chem.* 2004; 279:163–8. [PubMed: 14570928]
 31. Boo YC, Sorescu G, Boyd N, Shiojima I, Walsh K, Du J, Jo H. Shear stress stimulates phosphorylation of endothelial nitric-oxide synthase at Ser1179 by Akt-independent mechanisms: role of protein kinase A. *J Biol Chem.* 2002; 277:3388–96. [PubMed: 11729190]
 32. Dekker RJ, Boon RA, Rondaij MG, Kragt A, Volger OL, Elderkamp YW, Meijers JCM, Voorberg J, Pannekoek H, Horrevoets AJG. KLF2 provokes a gene expression pattern that establishes functional quiescent differentiation of the endothelium. *Blood.* 2006; 107:4354–63. [PubMed: 16455954]
 33. Dekker RJ, van Thienen JV, Rohlena J, de Jager SC, Elderkamp YW, Seppen J, de Vries CJM, Biessen EAL, van Berkel TJC, Pannekoek H, Horrevoets AJG. Endothelial KLF2 links local arterial shear stress levels to the expression of vascular tone-regulating genes. *Am J Pathol.* 2005; 167:609–18. [PubMed: 16049344]
 34. Fledderus JO, van Thienen JV, Boon RA, Dekker RJ, Rohlena J, Volger OL, Bijmens A-PJJ, Daemen MJAP, Kuiper J, van Berkel TJC, Pannekoek H, Horrevoets AJG. Prolonged shear stress and KLF2 suppress constitutive proinflammatory transcription through inhibition of ATF2. *Blood.* 2007; 109:4249–57. [PubMed: 17244683]
 35. Boon RA, Leyen TA, Fontijn RD, Fledderus JO, Baggen JMC, Volger OL, van Nieuw Amerongen GP, Horrevoets AJG. KLF2-induced actin shear fibers control both alignment to flow and JNK signaling in vascular endothelium. *Blood.* 2010; 115:2533–42. [PubMed: 20032497]
 36. Parmar KM, Nambudiri V, Dai G, Larman HB, Gimbrone MA, García-Cardena G. Statins exert endothelial atheroprotective effects via the KLF2 transcription factor. *J Biol Chem.* 2005; 280:26714–9. [PubMed: 15878865]
 37. Eden E, Navon R, Steinfeld I, Lipson D, Yakhini Z. GOrilla: a tool for discovery and visualization of enriched GO terms in ranked gene lists. *BMC Bioinformatics.* 2009; 10:48. [PubMed: 19192299]

38. Van Keulen JK, Timmers L, van Kuijk LP, Retnam L, Hoefler IE, Pasterkamp G, Lim SK, de Kleijn DPV. The Nuclear Factor-kappa B p50 subunit is involved in flow-induced outward arterial remodeling. *Atherosclerosis*. 2009; 202:424–30. [PubMed: 18617174]
39. Castier Y, Ramkhalawon B, Riou S, Tedgui A, Lehoux S. Role of NF-kappaB in flow-induced vascular remodeling. *Antioxid Redox Signal*. 2009; 11:1641–9. [PubMed: 19320561]
40. Tirziu D, Jaba IM, Yu P, Larrivé B, Coon BG, Cristofaro B, Zhuang ZW, Lanahan AA, Schwartz MA, Eichmann A, Simons M. Endothelial nuclear factor- κ B-dependent regulation of arteriogenesis and branching. *Circulation*. 2012; 126:2589–600. [PubMed: 23091063]
41. Toyota E, Warltier DC, Brock T, Ritman E, Kolz C, O'Malley P, Rocic P, Focardi M, Chilian WM. Vascular endothelial growth factor is required for coronary collateral growth in the rat. *Circulation*. 2005; 112:2108–13. [PubMed: 16203926]
42. Babiak A, Schumm A-M, Wangler C, Loukas M, Wu J, Dombrowski S, Matuschek C, Kotzerke J, Dehio C, Waltenberger J. Coordinated activation of VEGFR-1 and VEGFR-2 is a potent arteriogenic stimulus leading to enhancement of regional perfusion. *Cardiovasc Res*. 2004; 61:789–95. [PubMed: 14985076]
43. Hayashi S, Morishita R, Nakamura S, Yamamoto K, Moriguchi A, Nagano T, Taiji M, Noguchi H, Matsumoto K, Nakamura T, Higaki J, Ogihara T. Potential role of hepatocyte growth factor, a novel angiogenic growth factor, in peripheral arterial disease: downregulation of HGF in response to hypoxia in vascular cells. *Circulation*. 1999; 100:II301–308. [PubMed: 10567320]
44. Taniyama Y, Morishita R, Aoki M, Nakagami H, Yamamoto K, Yamazaki K, Matsumoto K, Nakamura T, Kaneda Y, Ogihara T. Therapeutic angiogenesis induced by human hepatocyte growth factor gene in rat and rabbit hindlimb ischemia models: preclinical study for treatment of peripheral arterial disease. *Gene Ther*. 2001; 8:181–9. [PubMed: 11313789]
45. Van Royen N, Hoefler I, Buschmann I, Heil M, Kostin S, Deindl E, Vogel S, Korff T, Augustin H, Bode C, Piek JJ, Schaper W. Exogenous application of transforming growth factor beta 1 stimulates arteriogenesis in the peripheral circulation. *FASEB J*. 2002; 16:432–4. [PubMed: 11821255]
46. Masaki I, Yonemitsu Y, Yamashita A, Sata S, Tani M, Komori K, Nakagawa K, Hou X, Nagai Y, Hasegawa M, Sugimachi K, Sueishi K. Angiogenic gene therapy for experimental critical limb ischemia: acceleration of limb loss by overexpression of vascular endothelial growth factor 165 but not of fibroblast growth factor-2. *Circ Res*. 2002; 90:966–73. [PubMed: 12016262]
47. Fujii T, Yonemitsu Y, Onimaru M, Tani M, Nakano T, Egashira K, Takehara T, Inoue M, Hasegawa M, Kuwano H, Sueishi K. Nonendothelial mesenchymal cell-derived MCP-1 is required for FGF-2-mediated therapeutic neovascularization: critical role of the inflammatory/arteriogenic pathway. *Arterioscler Thromb Vasc Biol*. 2006; 26:2483–9. [PubMed: 16960104]
48. Ren B, Deng Y, Mukhopadhyay A, Lanahan AA, Zhuang ZW, Moodie KL, Mulligan-Kehoe MJ, Byzova TV, Peterson RT, Simons M. ERK1/2-Akt1 crosstalk regulates arteriogenesis in mice and zebrafish. *J Clin Invest*. 2010; 120:1217–28. [PubMed: 20237411]
49. Sarateanu CS, Retuerto MA, Beckmann JT, McGregor L, Carbray J, Patejunas G, Nayak L, Milbrandt J, Rosengart TK. An Egr-1 master switch for arteriogenesis: studies in Egr-1 homozygous negative and wild-type animals. *J Thorac Cardiovasc Surg*. 2006; 131:138–45. [PubMed: 16399305]
50. Kinnaird T, Stabile E, Zbinden S, Burnett MS, Epstein SE. Cardiovascular risk factors impair native collateral development and may impair efficacy of therapeutic interventions. *Cardiovasc Res*. 2008; 78:257–64. [PubMed: 18178573]
51. Senthilkumar A, Smith RD, Khitha J, Arora N, Veerareddy S, Langston W, Chidlow JH, Barlow SC, Teng X, Patel RP, Lefer DJ, Kevil CG. Sildenafil promotes ischemia-induced angiogenesis through a PKG-dependent pathway. *Arterioscler Thromb Vasc Biol*. 2007; 27:1947–54. [PubMed: 17585066]
52. Bir SC, Xiong Y, Kevil CG, Luo J. Emerging role of PKA/eNOS pathway in therapeutic angiogenesis for ischaemic tissue diseases. *Cardiovasc Res*. 2012; 95:7–18. [PubMed: 22492672]
53. Venkatesh PK, Pattillo CB, Branch B, Hood J, Thoma S, Illum S, Pardue S, Teng X, Patel RP, Kevil CG. Dipyridamole enhances ischaemia-induced arteriogenesis through an endocrine nitrite/nitric oxide-dependent pathway. *Cardiovasc Res*. 2010; 85:661–70. [PubMed: 20061326]

54. Chen Z, Rubin J, Tzima E. Role of PECAM-1 in arteriogenesis and specification of preexisting collaterals. *Circ Res.* 2010; 107:1355–63. [PubMed: 20930147]
55. Tzima E, Irani-Tehrani M, Kiosses WB, Dejana E, Schultz DA, Engelhardt B, Cao G, DeLisser H, Schwartz MA. A mechanosensory complex that mediates the endothelial cell response to fluid shear stress. *Nature.* 2005; 437:426–31. [PubMed: 16163360]
56. Sweet DT, Chen Z, Givens CS, Owens AP, Rojas M, Tzima E. Endothelial Shc regulates arteriogenesis through dual control of arterial specification and inflammation via the Notch and NF- κ B pathways. *Circ Res.* 2013; 113:32–39. [PubMed: 23661718]
57. Lan Q, Mercurius KO, Davies PF. Stimulation of transcription factors NF κ B and AP1 in ECs subjected to shear stress. *Biochem Biophys Res Commun.* 1994; 201:950–956. [PubMed: 8003036]
58. Gruionu G, Hoying JB, Pries AR, Secomb TW. Structural remodeling of mouse gracilis artery after chronic alteration in blood supply. *Am J Physiol Hear Circ Physiol.* 2005; 288:2047–2054.
59. Gruionu G, Hoying JB, Pries AR, Secomb TW. Structural remodeling of the mouse gracilis artery: coordinated changes in diameter and medial area maintain circumferential stress. *Microcirculation.* 2012; 19:610–618. [PubMed: 22587333]
60. Johnson C, Sung H-J, Lessner SM, Fini ME, Galis ZS. Matrix metalloproteinase-9 is required for adequate angiogenic revascularization of ischemic tissues: potential role in capillary branching. *Circ Res.* 2004; 94:262–8. [PubMed: 14670843]
61. Scholz D, Ziegelhoeffer T, Helisch A, Wagner S, Friedrich C, Podzuweit T, Schaper W. Contribution of arteriogenesis and angiogenesis to postocclusive hindlimb perfusion in mice. *J Mol Cell Cardiol.* 2002; 34:775–87. [PubMed: 12099717]
62. Deindl E, Buschmann I, Hoefer IE, Podzuweit T, Boengler K, Vogel S, van Royen N, Fernandez B, Schaper W. Role of ischemia and of hypoxia-inducible genes in arteriogenesis after femoral artery occlusion in the rabbit. *Circ Res.* 2001; 89:779–786. [PubMed: 11679407]
63. Ito WD, Arras M, Scholz D, Winkler B, Htun P, Schaper W. Angiogenesis but not collateral growth is associated with ischemia after femoral artery occlusion. *Am J Physiol Hear Circ Physiol.* 1997; 273:H1255–H1265.
64. Adamson RH, Sarai RK, Altangerel A, Clark JF, Weinbaum S, Curry F-RE. Microvascular permeability to water is independent of shear stress, but dependent on flow direction. *Am J Physiol Hear Circ Physiol.* 2013; 304:H1077–1084.
65. Melchior B, Frangos JA. Shear-induced endothelial cell-cell junction inclination. *Am J Physiol Cell Physiol.* 2010; 299:C621–9. [PubMed: 20554908]
66. Passerini AG, Milsted A, Rittgers SE. Shear stress magnitude and directionality modulate growth factor gene expression in preconditioned vascular endothelial cells. *J Vasc Surg.* 2003; 37:182–90. [PubMed: 12514598]
67. Wang C, Baker BM, Chen CS, Schwartz MA. Endothelial cell sensing of flow direction. *Arter Thromb Vasc Biol.* 2013; 33:2130–2136.
68. Tzima E. Role of small GTPases in endothelial cytoskeletal dynamics and the shear stress response. *Circ Res.* 2006; 98:176–85. [PubMed: 16456110]
69. McCue S, Dajnowiec D, Xu F, Zhang M, Jackson MR, Langille BL. Shear stress regulates forward and reverse planar cell polarity of vascular endothelium in vivo and in vitro. *Circ Res.* 2006; 98:939–46. [PubMed: 16527990]
70. Tzima E, Del Pozo MA, Kiosses WB, Mohamed SA, Li S, Chien S, Schwartz MA. Activation of Rac1 by shear stress in endothelial cells mediates both cytoskeletal reorganization and effects on gene expression. *EMBO J.* 2002; 21:6791–800. [PubMed: 12486000]
71. Imberti B, Morigi M, Zoja C, Angioletti S, Abbate M, Remuzzi A, Remuzzi G. Shear stress-induced cytoskeleton rearrangement mediates NF- κ B-dependent endothelial expression of ICAM-1. *Microvasc Res.* 2000; 60:182–8. [PubMed: 10964593]
72. Troidl K, Rüdiger I, Cai W-J, Mücke Y, Grosseckler L, Piotrowska I, Apfelbeck H, Schierling W, Volger OL, Horrevoets AJ, Grote K, Schmitz-Rixen T, Schaper W, Troidl C. Actin-binding rho activating protein (Abra) is essential for fluid shear stress-induced arteriogenesis. *Arterioscler Thromb Vasc Biol.* 2009; 29:2093–101. [PubMed: 19778941]

73. Yu J, deMuinck ED, Zhuang Z, Drinane M, Kauser K, Rubanyi GM, Qian HS, Murata T, Escalante B, Sessa WC. Endothelial nitric oxide synthase is critical for ischemic remodeling, mural cell recruitment, and blood flow reserve. *Proc Natl Acad Sci U S A*. 2005; 102:10999–1004. [PubMed: 16043715]
74. Park B, Hoffman A, Yang Y, Yan J, Tie G, Bagshahi H, Nowicki PT, Messina LM. eNOS affects both early and late collateral arterial adaptation and blood flow recovery after induction of hindlimb ischemia in mice. *J Vasc Surg*. 2010; 51:1–17. [PubMed: 20117492]
75. Lloyd PG, Yang HT, Terjung RL. Arteriogenesis and angiogenesis in rat ischemic hindlimb: role of nitric oxide. *Am J Physiol Hear Circ Physiol*. 2001; 281:H2528–38.
76. Mees B, Wagner S, Ninci E, Tribulova S, Martin S, van Haperen R, Kostin S, Heil M, de Crom R, Schaper W. Endothelial nitric oxide synthase activity is essential for vasodilation during blood flow recovery but not for arteriogenesis. *Arterioscler Thromb Vasc Biol*. 2007; 27:1926–33. [PubMed: 17556651]
77. Kassab GS. Scaling laws of vascular trees: of form and function. *Am J Physiol Hear Circ Physiol*. 2005; 290:894–903.

Significance

Collateral arteriogenesis is a fundamental, yet poorly understood, growth response that can compensate for perfusion loss in patients with peripheral arterial disease (PAD). We report here that collateral segments that are exposed to flow direction reversal after arterial occlusion exhibit markedly augmented and unusually permanent arteriogenesis. Motivated by the potential therapeutic significance of this unique response, we performed transcriptional profiling of endothelial cells exposed to biomimetic flow-reversal, observing a broad increase in significantly regulated pro-arteriogenic transcripts, including ICAM-1, KLF-2, and eNOS, and an enhanced activation of multiple upstream regulators and canonical signaling pathways. Ultimately, this study is the first to directly map a comprehensive genome-wide analysis of endothelial signaling pathway activation to an amplified and sustained in-vivo arteriogenesis response.

Author Manuscript

Author Manuscript

Author Manuscript

Author Manuscript

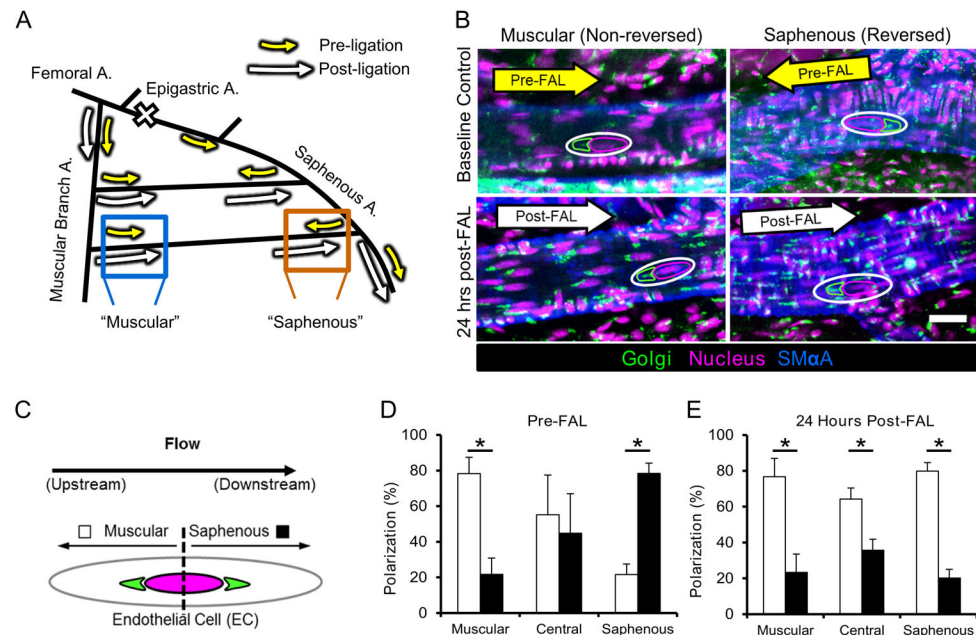


Fig. 1. Collateral artery endothelial cells repolarize in response to shear stress reversal after FAL

A) Schematic of the primary gracilis adductor collateral flow pathways after femoral arterial ligation (FAL). The femoral artery is ligated just distal to the epigastric artery thereby creating a change in flow direction at the saphenous branch entrance region. Arrows indicate the direction and magnitude of blood flow pre- (yellow) and post- (white) FAL. Flow magnitude increases in both the muscular branch and saphenous entrance regions, while flow direction also changes in the saphenous region. B) Representative images of collateral regions immunolabeled for the Golgi apparatus, the position of which was used to determine planar polarization, a marker of endothelial response to flow direction. Images are oriented such that the muscular branch is toward the left and the saphenous artery is toward the right. Arrows indicate blood flow direction. Note the upstream position of the Golgi apparatus (anti-giantin, outlined in green) with respect to the nucleus (Draq5, outline in magenta) (Scale bar=25 μ m). C) Diagram depicting the method used to quantify of polarization. The position of the Golgi apparatus (green) with respect to the nucleus (magenta) was used to classify EC polarization as toward either the saphenous (black bars) or muscular branch (white bars) arteries. D) Bar graph of pre-FAL EC planar polarization. ECs in the entrance regions show upstream polarization, while those central region show no directional bias (n=4). E) Bar graph of 24 hour post-FAL EC planar polarization. ECs in all regions show upstream polarization toward the muscular branch entrance region (n=4). *p<0.05 between muscular and saphenous polarization within the given region. Data are mean \pm SEM.

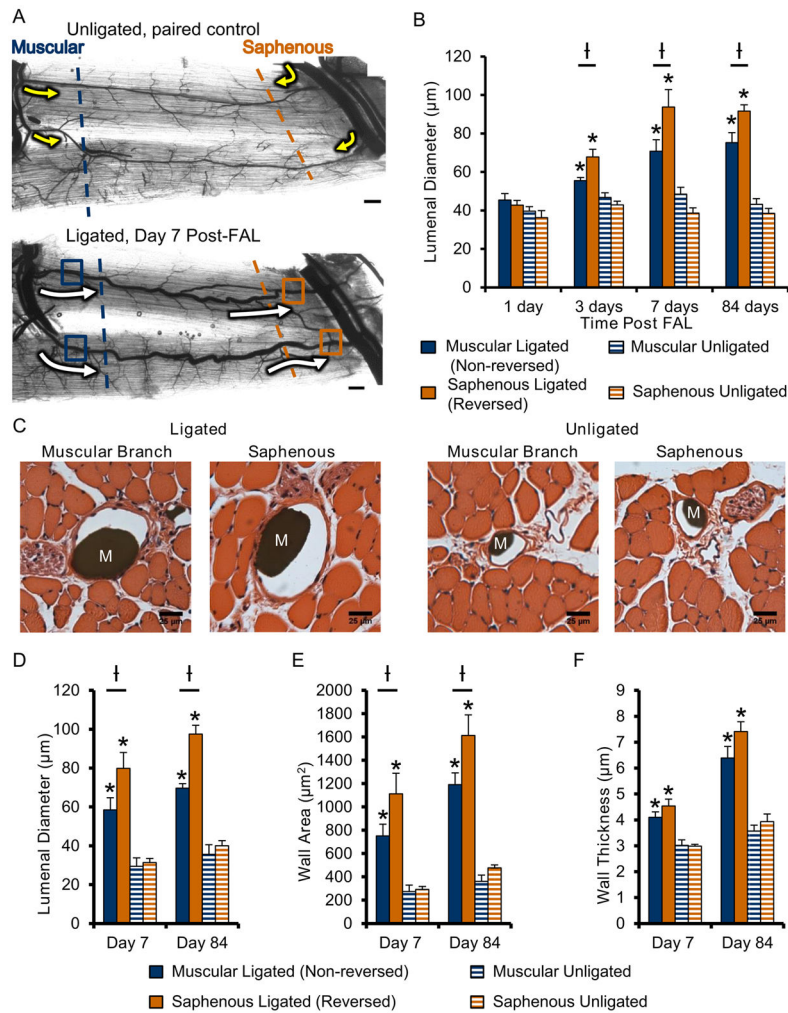


Fig. 2. Gracilis collateral artery regions exposed to flow-reversal exhibit enhanced arteriogenesis after FAL

A) Representative vascular cast images of gracilis collateral arteries from unligated sham control (top) and FAL-treated (bottom) mice. Arrows indicate the direction and relative magnitude of blood flow pre- (yellow) and post- (white) FAL. Dashed lines indicate the collateral artery region (muscular=blue; saphenous=orange) and approximate location where muscles were cut for regional cross-sectional analysis. Boxes indicate location at which luminal diameters were measured (i.e. near the first transverse arteriole branch point). B) Bar graph of collateral artery luminal diameter at both the non-reversed (muscular branch, blue) and flow-reversed (saphenous, orange) entrance regions. (n=6–7 mice per day). C) Representative H&E stained cross-sections of gracilis muscles. Microfil casting material (M) is evident in artery 7 lumens. D–F) Bar graphs of total cross sectional luminal diameter, wall area, and wall thickness (n=6–7 mice per day). *p<0.05 between ligated and unligated within the given region at the specified time-point; †p<0.05 between regions (i.e. saphenous vs. muscular) within the given treatment (i.e. ligated or unligated) at the specified time-point. Data are mean ± SEM.

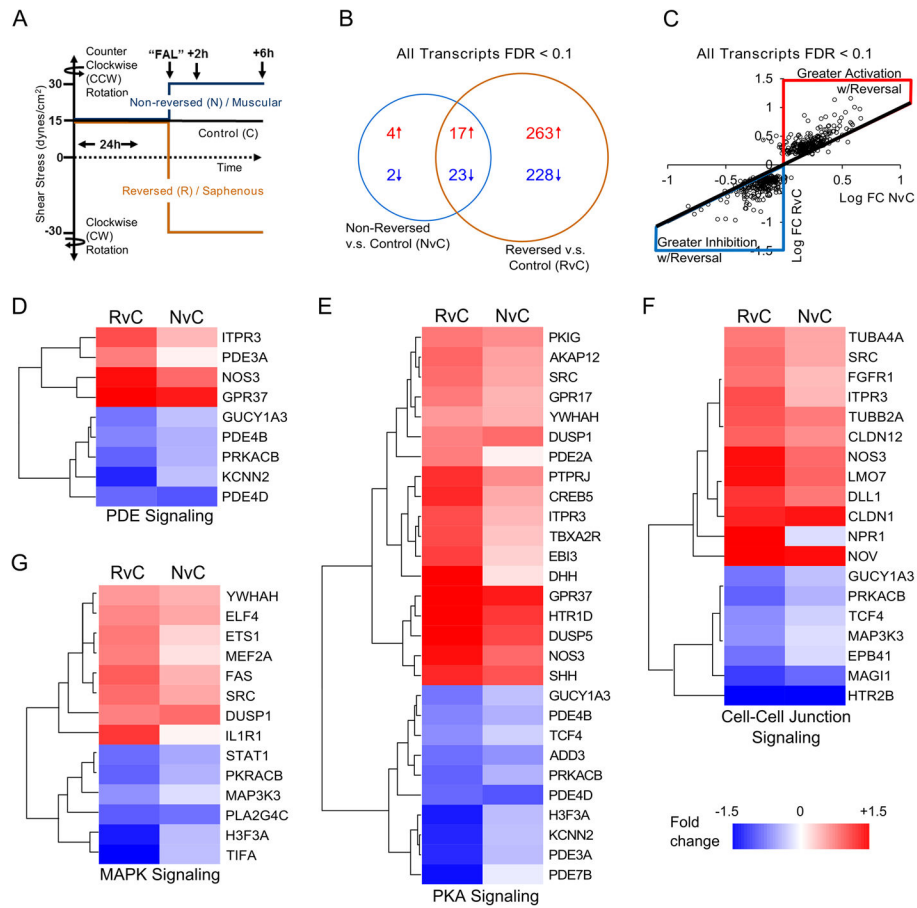


Fig. 3. Genome-wide analysis indicates that flow reversal broadly enhances the arteriogenic transcriptional profile

A) Schematic depicting shear stress conditions applied to HUVECs to simulate reversing (saphenous) and non-reversing (muscular) regions. HUVECs were preconditioned for 24 hours at 15 dynes/cm². Shear stress was then increased (or kept constant in the Control group) to 30 dynes/cm² in the same or opposite direction. B) Venn diagram of Affymetrix ST 1.0 human cDNA array data (n=4) comparing significantly altered transcripts (FDR<0.1) in non-reversed vs. control (NvC) conditions to those significantly altered with reversed direction vs. control (RvC). Red text and arrows=upregulated; Blue text and arrows=downregulated. C) Scatterplot showing gene expression changes between RvC and NvC conditions. While a similar overall pattern of expression (i.e. either up in both conditions or down in both conditions) was observed, gene expression was broadly amplified with the reversed shear stress condition (red region=greater up-regulation in RvC; blue region=greater down-regulation in RvC; black line=equal RvC and NvC). D–G) Heatmaps grouped along significantly altered canonical pathways (cell-cell junctional signaling, protein kinase A signaling, MAP kinase signaling, and phosphodiesterase signaling) activated in both RvC and NvC conditions (see Table S3A). Similar patterns of activation were observed between the conditions, but to a greater degree in the reversed flow condition.

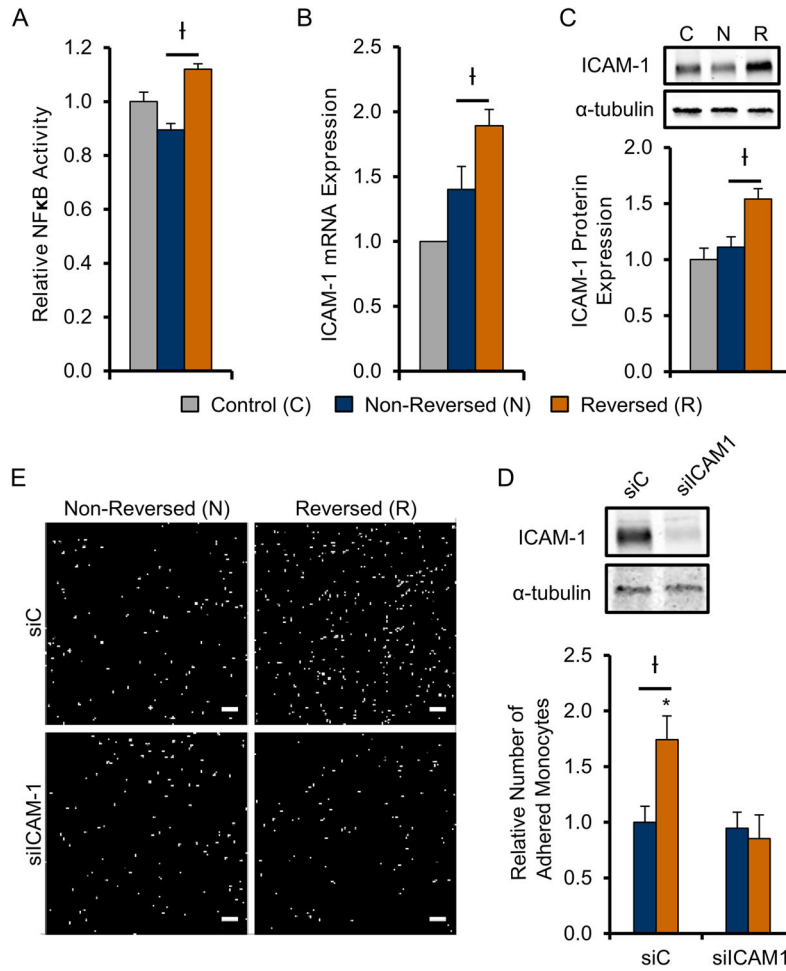


Fig. 4. Flow reversal enhances monocyte adhesion in-vitro in an ICAM-1 dependent manner
 A) NFκB activity (n=3) relative to control in HUVECs exposed to reversing (R, black) and non-reversing (N, white) shear conditions 1 hour post-“FAL” in vitro (Figure 3A). B, C) ICAM-1 mRNA expression by RT-PCR (n=8) and protein expression (n=4) in HUVECs relative to control 6 hours post in vitro “FAL”. D) Bar graph quantifying relative number of adhered monocytes in each condition E) Representative FOVs of THP-1 monocytes adhered to HUVECs exposed to reversed and non-reversed flow conditions transfected with either ICAM-1 siRNA (siICAM-1) or non-targeting control (siC) (Scale bar=100µm). †p<0.05 between reversing (R) and non-reversing (N);*p<0.05 between siC and siICAM-1 for given flow condition. Data are mean ± SEM.

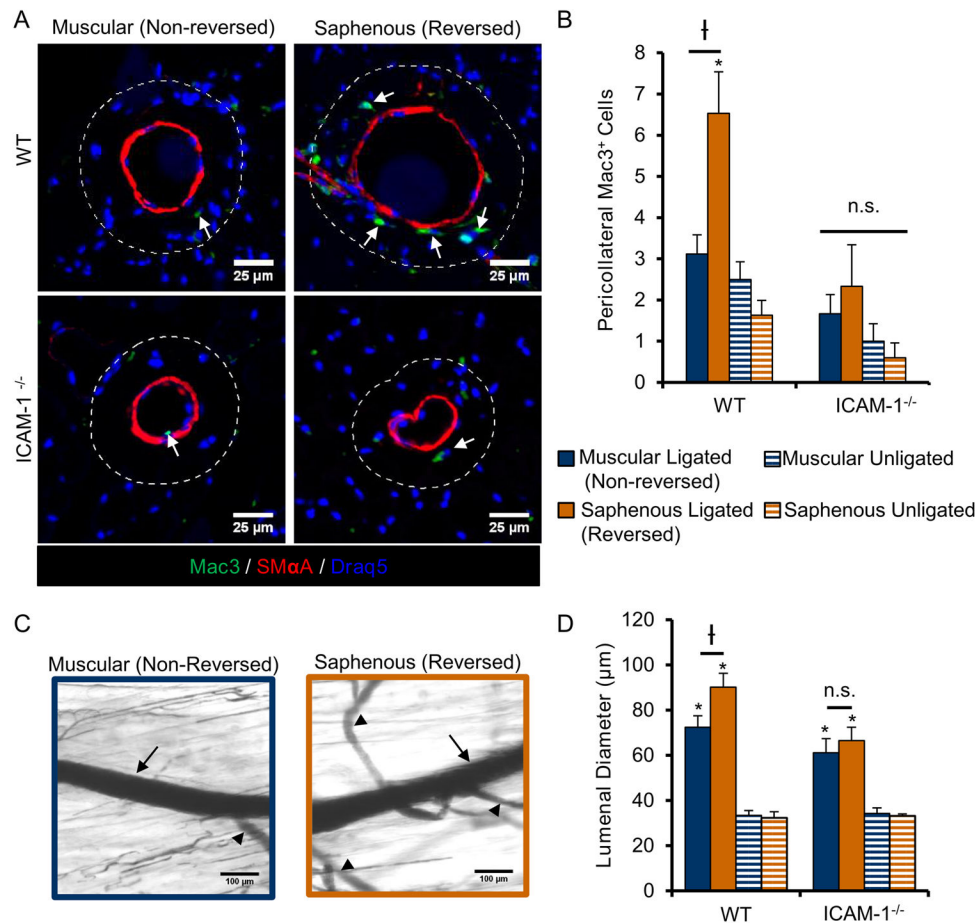


Fig. 5. ICAM-1 is necessary for enhanced macrophage recruitment and amplified arteriogenesis in collateral segments exposed to a flow reversal

A) Representative cross-sections of gracilis collateral artery regions in WT C57BL/6 and ICAM-1^{-/-} mice 3 days post-FAL immunolabeled for macrophage marker, Mac3 (green) and smooth muscle alpha actin (red). Dotted line indicates pericollateral region (25μm from vessel wall) used for quantification. Arrows indicate Mac3⁺ cells. (Scale bar=50μm) B) Bar graph of pericollateral Mac3⁺ cells. (n=4–5). C) Representative vascular cast images from ICAM^{-/-} mice 14 days post-FAL from both muscular and saphenous regions. (Scale bar=100μm). Arrows indicate the measured collateral artery while arrowheads indicate transverse arterioles. D) Bar graph of regional luminal diameter for both WT and ICAM-1^{-/-} mice (n=6). *p<0.05 between ligated and unligated within the given region; †p<0.05 between regions (saphenous versus muscular) within the given treatment (ligated or unligated). Data are mean ± SEM.

Table 1

Comparison of microarray genes to RT-PCR analyses for selected genes known to mediate arteriogenesis

Entrez Symbol	Gene Name	Comparison	RT-PCR Log ₂ Fold Change	Microarray		
				Log ₂ Fold Change	p-value	FDR
NOS3	nitric oxide synthase 3 (endothelial cell)	RvC	1.17 ± 0.49 ^{*†}	0.47 ± 0.13	2.03 e-5	0.011
		NvC	0.30 ± 0.44	0.29 ± 0.13	1.09 e-3	0.207
ICAM1	intercellular adhesion molecule 1	RvC	0.92 ± 0.25 ^{*†}	0.15 ± 0.12	0.031	0.331
		NvC	0.49 ± 0.44	0.10 ± 0.12	0.114	0.640
VCAM1	vascular cell adhesion molecule 1	RvC	0.23 ± 0.78	-0.22 ± 0.29	0.161	0.641
		NvC	-0.67 ± 0.43 [*]	-0.66 ± 0.29	9.86 e-4	0.203
KLF2	Kruppel-like factor 2 (lung)	RvC	0.84 ± 0.31 ^{*†}	0.33 ± 0.11	1.30 e-4	0.025
		NvC	0.43 ± 0.25 [*]	0.26 ± 0.11	7.47 e-4	0.176
KLF4	Kruppel-like factor 4 (gut)	RvC	0.95 ± 0.35 [*]	0.47 ± 0.13	1.86 e-5	0.010
		NvC	0.53 ± 0.33 [*]	0.26 ± 0.13	2.06 e-3	0.261
SELE	selectin E	RvC	-0.86 ± 0.63 [*]	-0.86 ± 0.32	2.57 e-4	0.032
		NvC	-0.94 ± 0.51 [*]	-0.77 ± 0.32	6.35 e-4	0.157
CCL2	chemokine (C-C motif) ligand 2	RvC	-0.69 ± 0.37 [*]	-0.19 ± 0.11	5.53 e-3	0.153
		NvC	-0.38 ± 0.32 [*]	-0.08 ± 0.11	0.168	0.706

Data represents RT-PCR (n=8/group) and microarray analysis (n=4/group). RvC, reversal versus control. NvC non-reversal versus control.

* indicates p<0.05 significance versus control RT-PCR.

† indicates significance p<0.05 of reversal v non-reversal by RT-PCR expression levels. Uncertainty in PCR is mean ± standard deviation for microarray mean ± 95% confidence

Table 2

NFκB is a predicted upstream regulator of gene expression patterns seen with flow reversed increased shear stress

Upstream Regulator	Reversal v Control		Non-reversal v Control	
	Activation Z-Score	p-value overlap	Activation Z-Score	p-value overlap
<i>I. NFκB Pathway</i>				
phorbol myristate acetate (activator PKC and NFκB)	2.767	1.35E-03		
NFKBIA	2.273	2.56E-02		4.95E-02
RELA	1.85	1.54E-02		
NFκB (complex)	1.47	3.99E-03		
IKKBK	1.272	6.94E-06		1.22E-02

All matching upstream regulators fitting into the defined groups with activation |z-score|>1.0

Author Manuscript

Author Manuscript

Author Manuscript

Author Manuscript